Numerical Investigation of Frontal Impact Response in an E-Rickshaw Chassis Using ANSYS Explicit Dynamics

Manan Sachdeva[1], Nipun Kothare[2]
mananslˆ717@gmail.com

ABSTRACT

The frontal crash response of lightweight electric rickshaw (E-rickshaw) chassis structures remains an important area for numerical investigation. This study examined the impact response of a simplified tubular E-rickshaw chassis using ANSYS Workbench 2026 R1 Explicit Dynamics. Two frontal impact velocities, 18 km/h (5 m/s) and 36 km/h (10 m/s), were investigated against a stationary rigid barrier over a simulation duration of 75 ms. The 18 km/h case was evaluated using total displacement and equivalent von Mises stress contours, while the model-wide maximum stress-time histories were compared for both velocities. The displacement contours indicated that the response extended from the frontal tubular members into the lower chassis, vertical supports, roof frame, and passenger-compartment framework. The maximum recorded total displacement was approximately 1.66 mm; however, this quantity includes rigid-body motion and cannot be interpreted directly as structural crushing or occupant-compartment intrusion. The maximum numerical equivalent von Mises stresses reached approximately 1.98 GPa and 4.60 GPa for the 18 km/h and 36 km/h cases, respectively, with the higher-speed case exhibiting an earlier peak. These unusually high stress magnitudes require further verification of the material representation and numerical model. The simplified chassis-only configuration, idealised connections, and limited crash-response outputs also restrict the interpretation of the findings. The study therefore provides a preliminary comparison of numerical impact responses and identifies structural regions warranting further investigation rather than establishing quantitative crashworthiness or occupant protection.

Keywords: *E-rickshaw, Explicit Dynamics, Finite Element Analysis, Frontal Impact Response, Impact Velocity, Von Mises Stress*

INTRODUCTION

Growth of Electric Rickshaws and Their Increasing Adoption

Electric rickshaws, commonly known as E-rickshaws, have rapidly emerged as one of the most widely adopted modes of last-mile transportation in India due to their affordability, low operating cost, and environmentally friendly operation (Priye & Manoj, 2020). Their adoption has been supported by

increasing demand for low-cost urban transport and the transition toward electric mobility (Chandran & Brahmachari, 2015).

A major reason for the popularity of E-rickshaws is their relatively low operating cost compared to conventional petrol and compressed natural gas auto-rickshaws. These economic advantages make E-rickshaws attractive for commercial drivers while also providing affordable mobility for passengers in dense urban and semi-urban areas (Cochrane et al., 2019).

Apart from economic benefits, E-rickshaws do not produce direct tailpipe emissions during operation and have therefore become an important component of the transition toward cleaner urban transport. As their usage continues to increase, structural safety and crashworthiness have become important engineering concerns that require systematic analysis (Singh et al., 2021).

Importance of Crashworthiness Assessment

Although E-rickshaws are now a major part of last-mile transport in India, their structural safety has not received the same level of attention as that of conventional passenger vehicles. The relatively lightweight and open construction of E-rickshaws raises important questions about their structural response during collisions, particularly because thin-walled structural geometry influences impact energy absorption and deformation behaviour (Reddy et al., 2018). Crashworthiness refers to the ability of a vehicle structure to absorb impact energy while preserving sufficient occupant survival space during a collision (Abramowicz, 2003). Excessive structural deformation can therefore adversely affect occupant protection (Gabauer & Juengprasertsak, 2022).

Safety assessment is especially important for three-wheeled vehicles because they operate alongside substantially larger vehicles in mixed traffic conditions. Real-world crash data from India have shown substantial injury burdens among motorised-rickshaw occupants and identified frontal collisions as particularly relevant to multiple-injury risk (Schmucker et al., 2011).

Vehicle Crash Testing and Virtual Crash Simulations

Vehicle crash testing is used to evaluate the structural response of vehicles under controlled impact conditions. During a frontal crash test, a vehicle impacts a barrier at a specified velocity while structural deformation and impact response are evaluated. Such tests provide important information about how loads are transferred through the vehicle structure during a collision (Kovandová et al., 2013).

Physical crash testing, however, is expensive and time-consuming, particularly when several structural configurations or impact conditions must be investigated. Finite element simulation provides an alternative approach in which vehicle deformation and stress response can be numerically studied under controlled impact conditions (Noorsumar et al., 2022).

Explicit finite element methods are particularly suitable for crash simulations because they can model large deformation, rapidly changing contact conditions, and highly nonlinear structural response during short-duration impacts (Danielson, 2022). Numerical crash simulations have therefore been widely applied to investigate frontal vehicle structures and identify regions of concentrated deformation and stress.

Finite Element Analysis and ANSYS Explicit Dynamics

Finite element analysis is widely used to investigate the structural response of vehicles under impact loading. In crashworthiness studies, the vehicle structure is discretized into finite elements so that deformation, stress distribution, and load transfer can be evaluated throughout the impact event. This allows critical structural regions to be identified without relying exclusively on physical crash testing (Huh & Kang, 2002).

Crash events involve large deformation, complex contact interactions, and rapidly changing structural response over very short time periods. Explicit finite element formulations are suited to highly nonlinear, transient impact problems involving rapidly changing contact conditions and structural response.

The accuracy of a finite element crash simulation also depends on factors such as mesh quality, contact definition, material representation, and boundary conditions (Salagame & Belegundu, 1994). Numerical studies have demonstrated that finite element modelling can be used to examine stress concentration, deformation patterns, and energy absorption in impact-loaded automotive structures (Marzbanrad et al., 2009).

Objectives of the Present Study

Existing research on vehicle crashworthiness demonstrates the importance of material behaviour, structural geometry, joint configuration, and numerical modelling assumptions in predicting impact response. However, findings obtained for conventional passenger vehicles or isolated energy-absorbing components cannot be transferred directly to lightweight tubular E-rickshaw chassis structures. The present study addresses this distinction by examining the numerical response of an interconnected E-rickshaw frame under two prescribed frontal impact velocities. Its contribution is limited to identifying regions of elevated numerical stress and describing the available displacement and stress-time responses. It does not establish a validated crashworthiness rating or quantify occupant protection.

The present study aims to numerically investigate the frontal crash response of a simplified E-rickshaw chassis using ANSYS Explicit Dynamics. The analysis focuses on the deformation and equivalent von Mises stress developed in the chassis during frontal impact against a rigid barrier. The study provides a

numerical assessment of structural response in a vehicle category for which crashworthiness has received comparatively limited research attention (Doley et al., 2023).

The specific objectives are to evaluate the progression of chassis deformation during frontal impact, identify regions of elevated equivalent von Mises stress, and compare the maximum stress response at impact velocities of 18 km/h and 36 km/h. The comparison is used to examine how increasing impact velocity influences the numerical structural response of the same chassis configuration.

METHODS

Overall Simulation Workflow

The frontal impact response of the E-rickshaw chassis was investigated through a numerical workflow comprising CAD model preparation, material assignment, finite element meshing, explicit dynamic simulation, and post-processing. A simplified three-dimensional model of the tubular chassis was prepared and imported into ANSYS Workbench 2026 R1. The model was discretised using tetrahedral elements, and mild-steel material properties were assigned through the Engineering Data library. The simulation configuration consisted of an initially moving chassis impacting a stationary rigid barrier, with the barrier constrained against translation and rotation.

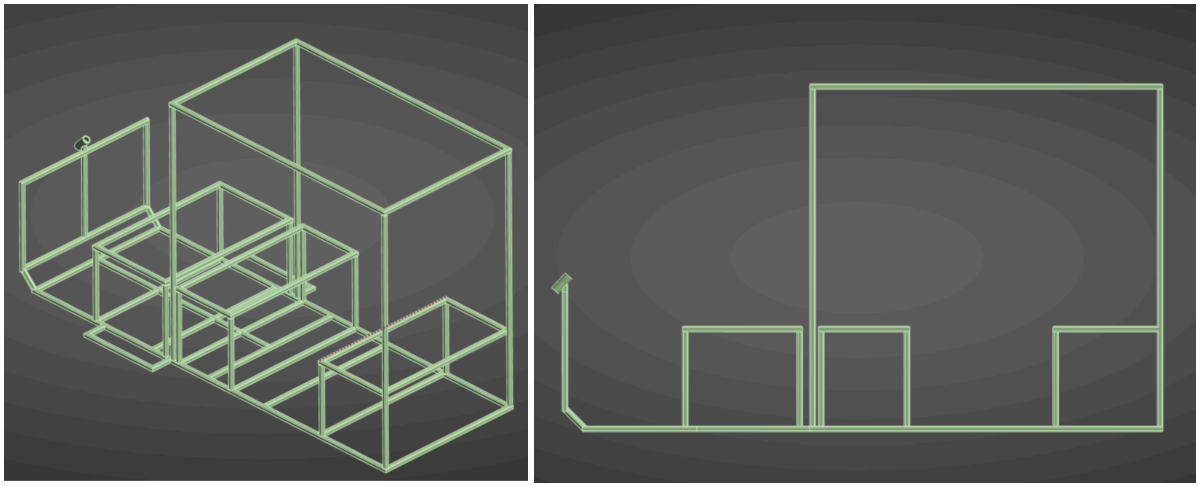
Two impact conditions were investigated by assigning initial chassis velocities of 5 m/s (18 km/h) and 10 m/s (36 km/h). The same chassis geometry, mesh, material assignment, contact definition, and analysis duration were maintained for both simulations to isolate the influence of the prescribed initial velocity on the recorded numerical response. Automatic body interaction with frictionless contact was used, and each simulation was conducted over a total duration of 75 ms.

The results were post-processed to examine total displacement and equivalent von Mises stress. For the 18 km/h case, spatial contours were evaluated at selected time points to investigate the progression of the impact response through the chassis framework. For both impact velocities, the model-wide maximum equivalent von Mises stress-time histories were compared to assess differences in the magnitude and timing of the numerical stress response. Because the available outputs do not quantify structural crushing, energy absorption, or passenger-compartment intrusion, the workflow provides a preliminary assessment of numerical impact behaviour rather than a complete crashworthiness evaluation.

CAD Model Preparation

The CAD model used in this investigation represents the primary tubular frame of an E-rickshaw. Hollow square-section structural members with outer dimensions of 20 mm × 20 mm and a uniform wall thickness of 2 mm were used to construct the chassis. The model includes the lower chassis frame, front driver compartment, passenger seating area, roof-support structure, vertical pillars, and rear frame

members. Non-structural components, including body panels, wheels, suspension components, seats, batteries, lighting systems, and interior fittings, were excluded to focus the analysis on the main structural framework. The chassis geometry was documented using isometric and side views, as presented in Figure 1. Although the member cross-sectional dimensions and wall thickness are specified, complete overall chassis dimensions and total structural mass are not reported. These omissions limit independent reproduction of the model.



(a) (b)

Figure 1. CAD model of the simplified E-rickshaw chassis used for crash simulation: (a) isometric view showing the overall tubular frame structure; (b) side view illustrating the longitudinal arrangement of the chassis members.

Shared topology was applied to the chassis geometry to establish continuous connectivity between intersecting tubular members. This approach allowed loads to be transferred through the interconnected frame without explicitly modelling individual welded connections. Consequently, the joints represent idealised continuous structural connections rather than detailed weld geometries. Local joint flexibility, weld failure, and potential separation between structural members were not independently evaluated.

The simulations considered a chassis-only configuration without explicit wheel-ground interaction or suspension support. The chassis was assigned an initial velocity towards the stationary rigid barrier, allowing its motion and structural response to develop during the impact event. This simplified configuration isolates the response of the tubular framework but does not reproduce the complete mass distribution, support conditions, or dynamic behaviour of an assembled E-rickshaw. The resulting displacement and stress fields should therefore be interpreted within the limitations of the idealised structural model.

Material Properties

Mild Steel was assigned to the E-rickshaw chassis using the ANSYS Workbench 2026 R1 Engineering Data library. The material was assumed to be homogeneous and isotropic. The specified properties included a density of 7850 kg/m³, Young's modulus of 200 GPa, Poisson's ratio of 0.30, tensile and compressive yield strengths of 250 MPa, and tensile ultimate strength of 460 MPa. The material was selected to represent the steel tubular members used in the simplified chassis model.

Although yield strength and ultimate tensile strength were included in the assigned material data, their presence in the Engineering Data library does not independently establish that plastic yielding or material failure was represented in the Explicit Dynamics solution. The available simulation documentation does not confirm whether an elastoplastic constitutive law, strain-rate-dependent plasticity, or a failure criterion was activated. Consequently, the material behaviour implemented by the solver must be verified before the numerical results can be interpreted as a physically representative crash response.

The reported equivalent von Mises stresses substantially exceed the assigned yield and ultimate tensile strengths. These magnitudes raise concerns regarding the adequacy of the material representation and cannot be used to establish realistic structural failure or crashworthiness performance without further verification. An appropriate elastoplastic material model, supported by documented constitutive parameters and relevant strain-rate behaviour, is required for a more reliable assessment of the chassis response under impact loading.

Mesh Generation

A three-dimensional tetrahedral mesh was used to discretise the E-rickshaw chassis geometry. Tetrahedral elements were selected to accommodate the numerous intersecting tubular members and structural connections, which would make the generation of a fully structured hexahedral mesh challenging. The resulting baseline mesh contained 63,005 nodes and 121,604 elements. Figure 2 presents the discretised chassis geometry used for the Explicit Dynamics simulations.

Although tetrahedral elements facilitated meshing of the interconnected tubular geometry, their suitability for representing thin-walled structural members under impact loading requires additional verification. In particular, solid-element models with insufficient discretisation through the wall thickness may inaccurately represent local bending and deformation. Shell elements offer an alternative formulation for thin-walled structures and should be considered in subsequent analyses. Since the number of elements through the tube wall thickness was not documented, the present mesh cannot be considered independently verified for thin-wall bending behaviour.

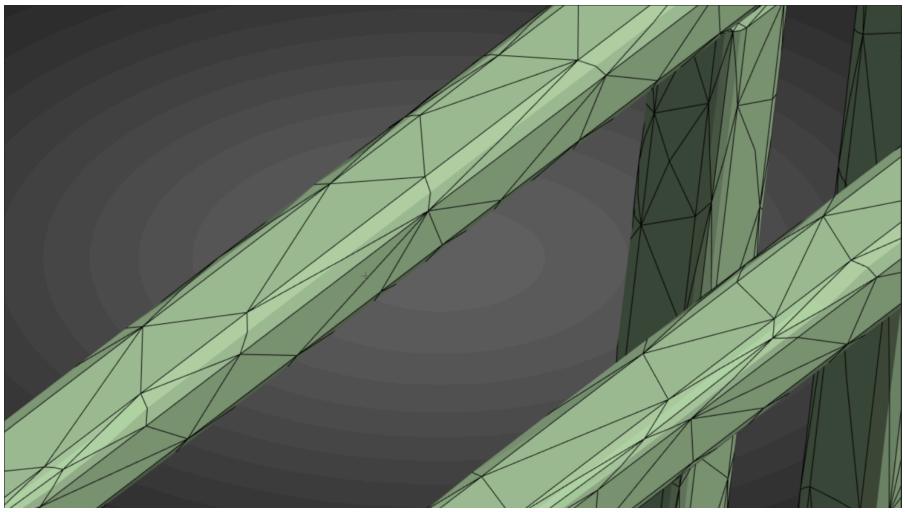


Figure 2. Finite element mesh of the E-rickshaw chassis generated using tetrahedral elements prior to Explicit Dynamics analysis.

Mesh quality was evaluated using the skewness metric available in ANSYS Mechanical. The baseline mesh had an average skewness of 0.52, a maximum skewness of 0.87, and a standard deviation of 0.37. These values provide an indication of element shape quality but do not independently establish the accuracy or convergence of the numerical impact response. The reliability of the calculated stresses also depends on the element formulation, local mesh resolution, contact representation, and constitutive material model.

A mesh-sensitivity assessment was conducted for the 18 km/h frontal impact case. The selected mesh employed a characteristic element size of 0.5 mm and produced a maximum equivalent von Mises stress of 1,984 MPa. Refinement to an element size of 0.1 mm produced a corresponding maximum stress of 1,952 MPa, representing a relative difference of 1.61% with respect to the selected mesh. This small difference suggests limited sensitivity of the reported peak stress to the investigated refinement. The 0.5 mm mesh was therefore retained for the comparative simulations. However, the assessment does not independently establish convergence of other response quantities, including global displacement, contact force, or absorbed energy.

Explicit Dynamics Simulation Setup

Frontal impact simulations were performed using the Explicit Dynamics module in ANSYS Workbench 2026 R1. The explicit solution approach was selected to model the rapidly changing contact conditions and transient structural response associated with frontal impact. A stationary rigid barrier was positioned directly in front of the E-rickshaw chassis and constrained using a fixed support to prevent translation and rotation. The chassis was left unconstrained and assigned an initial velocity directed towards the barrier. The rigid barrier was positioned perpendicular to the prescribed direction of chassis motion, facing the

frontal tubular members. Its exact height and width were not recorded in the available model documentation and therefore remain unverified.

An initial separation of 7.5 mm was maintained between the chassis and the barrier to prevent geometric overlap at the beginning of the simulation. Contact was defined using automatic body interaction with a frictionless contact formulation. This assumption excluded tangential frictional forces at the contact interface, allowing the numerical response to be examined under idealised normal contact conditions. However, frictionless contact may influence the predicted load distribution, sliding behaviour, and rotation of the chassis during impact. The structural connections within the chassis were represented through shared topology rather than explicitly modelled welds.

Each simulation was conducted as a single-step Explicit Dynamics analysis with a total duration of 75 ms. Stable time increments were determined automatically by the solver based on the finite element discretisation, material properties, and evolving structural conditions. The selected duration provided a common observation window for both impact velocities, although the available results do not independently demonstrate that all relevant impact and rebound processes had concluded by 75 ms.

Based on the initial separation of 7.5 mm and the prescribed chassis velocities, the estimated times to first contact are approximately 1.5 ms for the 18 km/h case and 0.75 ms for the 36 km/h case, assuming constant velocity before impact. The 75 ms simulation duration was selected to provide a common observation interval extending well beyond the estimated onset of contact for both impact conditions. However, the available results do not establish the precise time of contact termination or rebound. Consequently, the selected analysis duration should be interpreted as the observation window rather than confirmation that the complete collision and rebound processes were captured.

For the 18 km/h simulation, displacement and equivalent von Mises stress contours were evaluated at 18.75 ms, 37.50 ms, 56.25 ms, and 75.00 ms, corresponding to 25%, 50%, 75%, and 100% of the analysis duration. The 36 km/h simulation used the same geometry, mesh, material assignment, barrier configuration, initial separation, contact conditions, and analysis settings. Initial velocity was the only parameter intentionally varied between the two cases, enabling a controlled comparison of their recorded numerical stress responses.

Frontal Impact Cases

Two frontal impact conditions were investigated to compare the numerical response of the E-rickshaw chassis at different initial velocities. The first simulation used an initial velocity of 18 km/h (5 m/s), while the second used 36 km/h (10 m/s). These values were selected to establish a controlled comparison between a lower-velocity and a higher-velocity impact, with the initial velocity doubled between the two

cases. The selected speeds represent comparative numerical loading conditions and should not be interpreted as independently validated regulatory crash-test scenarios.

The two impact velocities were selected to examine the structural response under contrasting frontal impact conditions. The lower velocity of 18 km/h represents a low-speed collision within the nominal 25 km/h maximum design-speed limit applicable to Indian e-rickshaws. The higher velocity of 36 km/h was selected as an elevated-impact scenario to investigate the sensitivity of the chassis response to increased collision severity. It exceeds the nominal design-speed limit and is therefore treated as a hypothetical comparative loading condition rather than a representative normal operating speed or a standard regulatory crash-test condition.

In the 18 km/h case, the structural response was examined using total displacement and equivalent von Mises stress contours at four selected time points: 18.75 ms, 37.50 ms, 56.25 ms, and 75.00 ms. These outputs were used to identify the regions exhibiting the greatest recorded movement and elevated numerical stress during the impact. The model-wide maximum equivalent von Mises stress was also recorded over the analysis duration to characterise its temporal variation.

The 36 km/h case was conducted using the same chassis geometry, material assignment, finite element mesh, rigid-barrier configuration, initial separation, contact definition, boundary conditions, and analysis duration. The initial chassis velocity was the only parameter intentionally varied. For this case, the available analysis focused on the model-wide maximum equivalent von Mises stress-time history, which was compared with the corresponding result from the 18 km/h simulation. Detailed spatial displacement and stress contours were not evaluated for the higher-velocity case.

For an unchanged chassis mass, doubling the initial velocity increases the initial kinetic energy by a factor of four. However, this relationship does not imply a corresponding fourfold increase in equivalent von Mises stress, structural deformation, or absorbed energy. The simulations were therefore compared using their recorded numerical stress responses without assuming a proportional relationship between velocity and structural damage. The common simulation parameters are summarised in Table 1.

As a preliminary analytical check, the one-dimensional elastic stress-wave relation $\sigma = \rho c v$ was considered, where ρ is material density, c is the longitudinal wave-speed approximation $\sqrt{(E/\rho)}$, and v is impact velocity. Using the assigned mild-steel density of 7850 kg/m^3 and Young's modulus of 200 GPa gives an approximate wave speed of 5050 m/s. The corresponding nominal stress estimates are approximately 198 MPa at 5 m/s and 396 MPa at 10 m/s. These estimates are comparable to or greater than the assigned yield strength of 250 MPa, indicating that plasticity may become important, particularly in the higher-velocity case. The calculation is an idealised one-dimensional

estimate rather than a prediction of local stresses in the three-dimensional chassis, and it cannot validate the much larger numerical peak stresses reported in the simulations.

Table 1. Simulation parameters for the frontal impact analysis

Parameter	Value
Software	ANSYS Workbench 2026 R1
Analysis	Explicit Dynamics
Impact velocities	18 km/h and 36 km/h
Simulation duration	75 ms
Initial chassis–barrier gap	7.5 mm
Contact	Frictionless
Chassis material	Mild Steel
Density	7850 kg/m³
Young's modulus	200 GPa
Poisson's ratio	0.30
Yield strength	250 MPa
Ultimate tensile strength	460 MPa
Tube cross-section	20 × 20 mm
Tube wall thickness	2 mm
Mesh	Tetrahedral
Nodes	63,005
Elements	121,604
Average skewness	0.52

Output Parameters

Total displacement and equivalent von Mises stress were evaluated using ANSYS Explicit Dynamics to characterise the numerical response of the E-rickshaw chassis during frontal impact. For the 18 km/h simulation, displacement contours were examined at 18.75 ms, 37.50 ms, 56.25 ms, and 75.00 ms to assess the progression of the impact response through the tubular framework. Equivalent von Mises stress contours were also examined at these time points to identify regions of elevated numerical stress and changes in their spatial distribution.

Total displacement represents the magnitude of nodal movement relative to the initial configuration. Because the chassis was unconstrained during the impact simulation, this quantity includes rigid-body translation and rotation as well as structural deformation. It was therefore used to describe the overall movement of the chassis rather than to quantify local crushing, permanent deformation, or passenger-compartment intrusion. Equivalent von Mises stress was used to examine the distribution of numerical stress within the structural members, although its physical interpretation depends on the constitutive material model and numerical accuracy of the simulation.

For the comparison between impact velocities, the model-wide maximum equivalent von Mises stress was recorded over the 75 ms analysis duration for both the 18 km/h and 36 km/h cases. The resulting stress-time histories were used to compare the magnitude and timing of the recorded peak stresses. Because the maximum value at each time point may occur at a different location within the chassis, these histories represent the evolution of the global maximum rather than the stress history of a single element or material point.

The available output set did not include quantified structural intrusion, plastic deformation, absorbed energy, or contact-force histories. Consequently, the analysis was restricted to examining displacement patterns, numerical stress distributions, and differences between the recorded maximum stress-time responses. These outputs provide a preliminary description of the simulated impact behaviour but are insufficient for a comprehensive quantitative assessment of crashworthiness.

RESULTS

The numerical results were examined to characterise the response of the simplified E-rickshaw chassis during frontal impact against a stationary rigid barrier. For the 18 km/h (5 m/s) simulation, total displacement and equivalent von Mises stress contours were evaluated at 18.75 ms, 37.50 ms, 56.25 ms, and 75.00 ms. These four time points represent successive stages within the 75 ms analysis duration and provide a basis for examining changes in the spatial distribution of the recorded response.

Total displacement contours were used to examine the movement of the frontal members and surrounding chassis framework, while equivalent von Mises stress contours were used to identify regions of elevated numerical stress. Because the chassis was unconstrained, the displacement results include rigid-body motion as well as structural deformation. The spatial results from the 18 km/h simulation were supplemented by a comparison of the model-wide maximum equivalent von Mises stress-time histories for the 18 km/h and 36 km/h impact cases. Together, these outputs provide a preliminary description of the numerical impact response, subject to the limitations of the simplified geometry, material representation, and available simulation measurements.

Total Deformation Response

At 18.75 ms, the displacement contours are primarily concentrated around the frontal tubular members that come into direct contact with the rigid barrier, as shown in Figure 3(a). The frontal members exhibit visible bending, while the lower chassis and passenger-compartment framework experience comparatively smaller displacements. This indicates that the initial impact response is most pronounced near the contact region before extending into the surrounding structural framework.

At 37.50 ms, the maximum recorded total displacement reaches approximately 1.66 mm, as shown in Figure 3(b). The displacement contours indicate movement extending beyond the frontal members into the roof frame, vertical supports, lower chassis, and passenger-compartment structure. The rear portion of the frame also exhibits upward rotation relative to its initial orientation, suggesting that rigid-body pitching contributes to the overall displacement response. Consequently, the reported maximum displacement should not be interpreted exclusively as structural deformation, since it includes translation and rotation of the unconstrained chassis.

At 56.25 ms, the maximum total displacement remains approximately 1.66 mm, as shown in Figure 3(c). The lower longitudinal members exhibit visible changes in curvature, while the roof and rear sections show substantial movement relative to their original positions. The passenger-compartment framework also displays changes in its overall configuration. Although the maximum displacement is nearly unchanged from the preceding stage, this similarity does not establish that structural deformation has ceased, because the reported quantity includes both rigid-body motion and deformation of the chassis.

At 75.00 ms, the maximum total displacement remains approximately 1.66 mm, as shown in Figure 3(d). The displacement contours indicate continued movement of the frontal structure, lower chassis, roof frame, rear members, and passenger-compartment framework, with visible changes in the orientation of several structural members. The maximum recorded displacement remains nearly unchanged between 37.50 ms and 75.00 ms. However, because total displacement includes rigid-body translation and rotation of the unconstrained chassis, this apparent plateau cannot independently establish whether structural deformation had ceased or whether the chassis had reached a stable configuration.

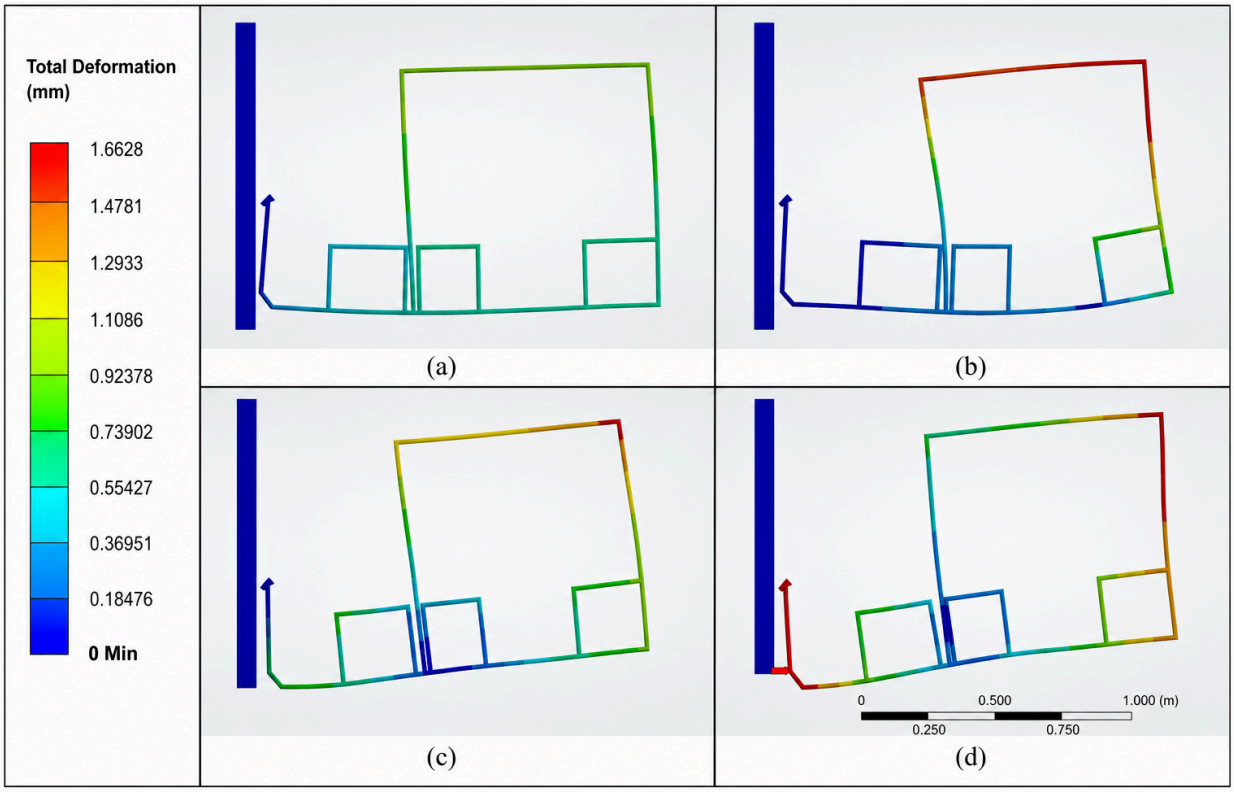


Figure 3. Progression of total deformation during the 18 km/h frontal impact at (a) 18.75 ms, (b) 37.50 ms, (c) 56.25 ms, and (d) 75.00 ms.

Overall, the displacement contours indicate that the chassis response extends from the frontal impact region into the surrounding structural framework. The frontal tubular members initially exhibit the most prominent displacement, followed by movement of the lower chassis, vertical supports, roof frame, rear members, and passenger-compartment structure. The progression of the contours illustrates how the impact response develops throughout the interconnected frame. However, because the reported total displacement includes rigid-body translation and rotation, the contours alone cannot establish the magnitude of local structural deformation or passenger-compartment intrusion.

The approximately 1.66 mm maximum total displacement is not a measure of frontal crush distance or passenger-compartment intrusion. A quantitative intrusion assessment would require tracking the relative positions of defined structural reference points, such as a frontal member and a passenger-compartment reference location, throughout the impact. Because these relative-displacement measurements were not included in the available output set, neither maximum crush distance nor intrusion can be determined from the reported total-displacement contours.

Equivalent von Mises Stress Response

At 18.75 ms, the maximum recorded equivalent von Mises stress was approximately 1.92 GPa. The highest numerical stresses were concentrated around the frontal tubular members and their connections to the main chassis, while much of the remaining structure exhibited comparatively lower stress magnitudes. The distribution identifies the frontal joints and intersecting structural members as regions of elevated local stress during the early impact response.

At 37.50 ms, the maximum equivalent von Mises stress decreased to approximately 1.20 GPa. Elevated stresses remained visible around the central vertical members and connections between the lower chassis and passenger-compartment framework. The changing distribution suggests that the numerical stress response extended beyond the initial contact region through the interconnected tubular structure.

At 56.25 ms, the maximum equivalent von Mises stress decreased further to approximately 0.871 GPa, the lowest value among the four selected contour stages. Localised regions of elevated stress remained near the frontal structure and the intersections between vertical and horizontal members. The reduction in the model-wide maximum stress did not necessarily indicate that the structural response had stabilised, since the displacement contours continued to show movement of the chassis.

By 75.00 ms, the maximum equivalent von Mises stress had increased to approximately 1.50 GPa, as shown in Figure 4. The highest recorded stress was concentrated near a frontal upper structural joint, while most other regions remained within lower ranges of the displayed contour. The increase from approximately 0.871 GPa at 56.25 ms indicates a non-monotonic numerical stress response during the later stages of the simulated impact.

The recorded stress magnitudes substantially exceed the assigned mild-steel yield strength of 250 MPa and ultimate tensile strength of 460 MPa. Consequently, these values cannot be interpreted as physically validated material stresses or direct evidence of structural failure without confirming the constitutive material model implemented in the solver. Local stress concentrations near contact interfaces, sharp geometric transitions, and structural intersections may also be sensitive to mesh discretisation and element formulation. The reported maxima therefore require further numerical verification, including an appropriate elastoplastic material representation and a documented convergence assessment.

Overall, the stress contours consistently identify the frontal tubular members and their connections to the main chassis as regions of elevated numerical stress. The variation in maximum stress across the selected time points demonstrates that the recorded response changes throughout the 75 ms simulation rather than decreasing continuously. However, the present results are most appropriately used to identify regions requiring further investigation, rather than to quantify material yielding, structural failure, or the crashworthiness of the E-rickshaw chassis.

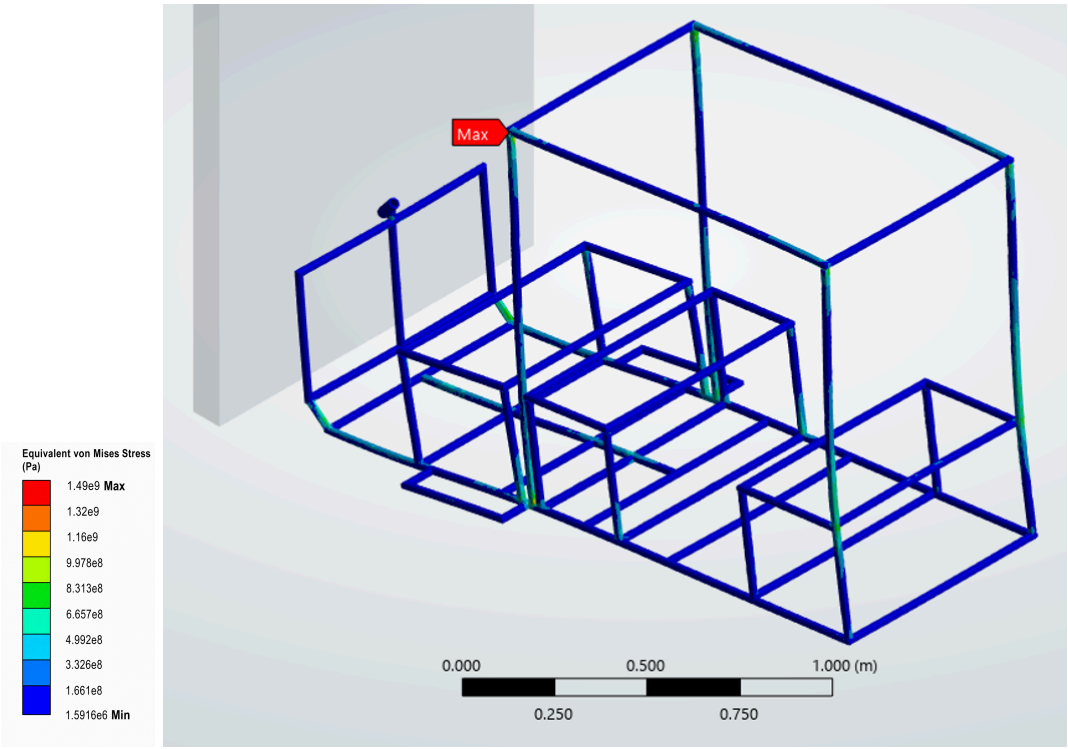


Figure 4. Equivalent von Mises stress distribution in the E-rickshaw chassis at 75 ms during the 18 km/h frontal impact simulation. The maximum numerical stress is indicated near a frontal upper structural joint. The ANSYS contour legend reports stress in pascals (Pa), whereas the accompanying discussion expresses stress in gigapascals (GPa).

Overall Chassis Structural Response

The total displacement and equivalent von Mises stress results provide complementary descriptions of the E-rickshaw chassis response during the 18 km/h frontal impact simulation. During the initial stages, the frontal tubular members experience direct contact with the rigid barrier and exhibit elevated numerical stresses and visible changes in their configuration. As the simulation progresses, the displacement contours show movement extending into the lower longitudinal members, vertical supports, roof frame, rear members, and passenger-compartment framework. These observations indicate that the simulated impact response involves several interconnected structural regions rather than remaining confined to the frontal contact area.

The displacement and stress contours exhibit different spatial patterns. Elevated equivalent von Mises stresses occur primarily around the frontal tubular members and their connections to the main chassis, whereas substantial total displacements are recorded across a broader portion of the structure. This distinction is important because the location of maximum numerical stress does not necessarily

correspond to the location of maximum displacement. Furthermore, the reported total displacement includes rigid-body translation and rotation of the unconstrained chassis. Consequently, the displacement contours cannot independently establish the magnitude of structural crushing, permanent deformation, or intrusion into the passenger compartment.

The observed stress concentrations suggest that connections between the frontal members, lower longitudinal rails, and adjacent vertical supports warrant further investigation. However, the unusually high recorded stress magnitudes require verification of the material constitutive model and numerical solution before they can be interpreted as physically meaningful indicators of yielding or structural failure. Similarly, the absence of quantified plastic deformation, internal-energy histories, and relative structural displacements prevents a definitive assessment of energy absorption or occupant survival space. The present results therefore provide a preliminary identification of potentially critical structural regions rather than a validated measure of chassis crashworthiness.

Effect of Increased Impact Velocity

The comparison of the model-wide maximum equivalent von Mises stress-time histories indicates a substantial difference in the numerical response of the E-rickshaw chassis when the initial impact velocity was increased from 18 km/h (5 m/s) to 36 km/h (10 m/s). For the 18 km/h simulation, the maximum recorded equivalent von Mises stress reached approximately 1.98 GPa at around 20 ms. In comparison, the 36 km/h simulation produced a higher recorded peak of approximately 4.60 GPa at around 15 ms. The peak stress at the higher velocity was approximately 2.32 times that of the lower-velocity case and occurred earlier in the impact event.

The stress-time histories presented in Figure 5 are based on discrete recorded output points rather than continuous measurements of the structural response. Consequently, the reported peak times represent the maxima among the available samples and should not be interpreted as the exact instants of peak stress. The spacing of the recorded points also limits the resolution of short-duration stress fluctuations, particularly around initial contact. The comparison is therefore restricted to the sampled numerical histories, and finer, synchronised output intervals would be required to establish more accurate peak magnitudes and timings.

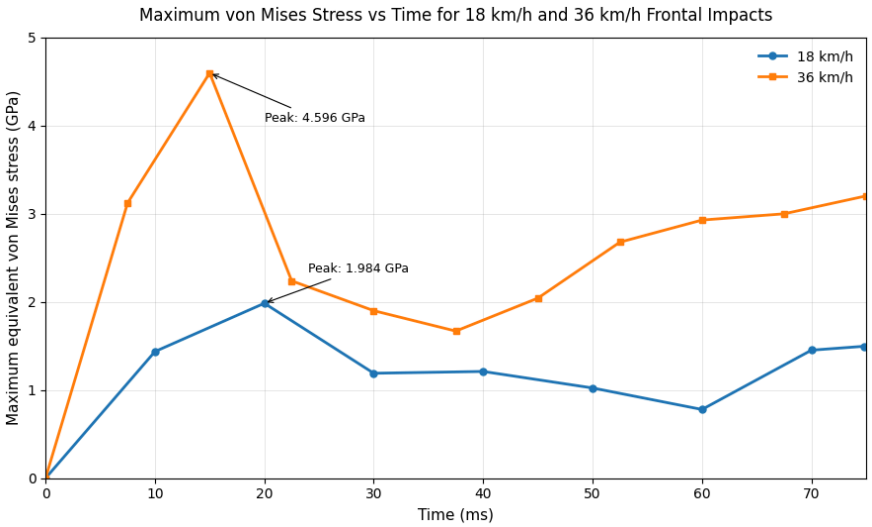


Figure 5. Comparison of the model-wide maximum equivalent von Mises stress over time for frontal impacts at 18 km/h and 36 km/h.

Following their respective peaks, the maximum equivalent von Mises stresses decreased in both simulations, although the higher-velocity case generally maintained greater recorded stress magnitudes. At approximately 75 ms, the maximum stress was about 3.20 GPa for the 36 km/h simulation, compared with approximately 1.50 GPa for the 18 km/h simulation. These results indicate that increasing the prescribed initial velocity affected both the magnitude and temporal development of the recorded numerical stress response. However, the model-wide maximum at each time point may occur at a different element or structural location, and the stress-time histories therefore do not necessarily represent the evolution of stress at a single material point.

Doubling the initial velocity increases the initial kinetic energy by a factor of four when the chassis mass remains unchanged. Nevertheless, the ratio between the recorded maximum stresses cannot be interpreted as a direct measure of kinetic energy absorption or structural damage. Equivalent von Mises stress depends on the material constitutive response, structural geometry, contact interactions, and local deformation conditions. Furthermore, the reported peak stresses exceed the assigned mild-steel yield and ultimate tensile strengths, making verification of the implemented material model essential before drawing quantitative conclusions about the influence of impact velocity.

The comparison is also limited by the available simulation outputs. Detailed spatial displacement and stress contours were evaluated for the 18 km/h case, whereas the 36 km/h case was assessed primarily through its model-wide maximum equivalent von Mises stress-time history. Consequently, the present analysis does not establish how the higher impact velocity affected structural crushing, passenger-compartment intrusion, plastic deformation, or absorbed energy. A more comprehensive comparison would require verified elastoplastic simulations and corresponding displacement,

contact-force, internal-energy, and plastic-work histories for both impact conditions.

Overall, the results demonstrate that the higher prescribed impact velocity produced a larger and earlier numerical peak stress under the investigated simulation settings. This finding supports a preliminary comparison of the two recorded stress responses but does not independently establish the relative crashworthiness or occupant protection provided by the chassis at either velocity.

DISCUSSION

The frontal impact simulations indicate that the numerical response of the E-rickshaw chassis extends beyond the initial contact region. In the 18 km/h case, elevated equivalent von Mises stresses were concentrated primarily around the frontal tubular members and their connections to the main chassis. The displacement contours also showed movement extending into the lower longitudinal members, vertical supports, roof structure, rear frame, and passenger-compartment framework. These observations suggest that the interconnected tubular structure transmits impact loads through multiple structural regions rather than confining the response to the frontal members.

The displacement results require careful interpretation because the chassis was unconstrained during the impact simulation. The reported maximum total displacement of approximately 1.66 mm includes rigid-body translation and rotation in addition to structural deformation. Consequently, this value cannot be interpreted directly as chassis crushing or passenger-compartment intrusion. Although the displacement contours indicate movement of the passenger-compartment framework, the present analysis does not quantify changes in occupant survival space. Relative displacement measurements between selected structural locations would be necessary to distinguish local deformation from overall chassis motion.

The equivalent von Mises stress contours identify the frontal structural joints and intersections between tubular members as regions of elevated numerical stress. Such locations are relevant to the investigation of impact load transfer because geometric transitions and structural connections can influence local stress distributions (Baykasoğlu et al., 2019). However, the maximum recorded stresses substantially exceed the assigned mild-steel yield strength of 250 MPa and ultimate tensile strength of 460 MPa. Their physical interpretation therefore depends on verification of the constitutive material model implemented in ANSYS Explicit Dynamics. Without confirming appropriate plasticity behaviour and assessing numerical convergence, these stress magnitudes cannot be treated as validated predictions of material yielding or structural failure.

The comparison between the 18 km/h and 36 km/h simulations indicates that increasing the initial impact velocity produces a larger and earlier recorded maximum equivalent von Mises stress. The higher-velocity simulation reached approximately 4.60 GPa at around 15 ms, compared with approximately 1.98 GPa at around 20 ms for the lower-velocity case. However, the ratio between these numerical peak stresses

should not be interpreted as a measure of energy absorption or structural damage. For an unchanged chassis mass, doubling the initial velocity increases the initial kinetic energy by a factor of four, but the resulting structural response depends on material behaviour, contact interactions, geometry, and deformation mechanisms.

The maximum stress-time histories also indicate that elevated numerical stresses persisted during the later stages of both simulations, particularly in the higher-velocity case. Nevertheless, the model-wide maximum stress may occur at different structural locations over time, limiting its usefulness as a measure of the loading history experienced by any individual component. Furthermore, the absence of corresponding contact-force, internal-energy, plastic-work, and structural-crushing histories prevents a quantitative assessment of how the initial kinetic energy was redistributed or absorbed during impact.

The numerical model incorporates several simplifications that influence the interpretation of these findings. The chassis-only configuration excludes wheels, suspension components, batteries, body panels, and occupants, while shared-topology connections idealise the behaviour of structural joints. The rigid-barrier impact and frictionless contact assumptions also differ from many real-world collision conditions. In addition, the available results do not provide sufficient evidence to establish mesh convergence across multiple response quantities or to validate the predicted behaviour against experimental observations. These limitations restrict the generalisability of the numerical results to complete E-rickshaw crash performance.

The analytical stress-wave estimate provides an order-of-magnitude plausibility check for the reported numerical stresses, but it does not constitute independent validation of the finite element model. The estimate assumes idealised one-dimensional elastic wave propagation and does not represent the three-dimensional geometry, local contact conditions, bending response, or material nonlinearity of the chassis. Accordingly, agreement or disagreement with this estimate cannot establish the accuracy of the simulated structural response. Experimental measurements or comparison with a suitably documented impact benchmark would be necessary for quantitative validation.

Despite these limitations, the simulations provide a preliminary indication of structural regions that warrant closer examination. The frontal tubular members, their intersections with the lower chassis, and adjacent vertical supports consistently appear important in the recorded stress distributions. Future work should investigate these regions using verified elastoplastic material models, documented mesh-convergence studies, and additional crash-response measurements. Evaluating alternative frontal structural configurations, together with absorbed energy, plastic deformation, contact forces, and passenger-compartment intrusion, would provide a stronger basis for assessing potential improvements in E-rickshaw crashworthiness.

CONCLUSION

This study investigated the frontal impact response of a simplified E-rickshaw chassis using ANSYS Explicit Dynamics at initial velocities of 18 km/h and 36 km/h. The displacement contours for the 18 km/h simulation indicated that the impact response extended beyond the frontal tubular members into the lower chassis, vertical supports, roof frame, and passenger-compartment framework. Elevated numerical equivalent von Mises stresses were concentrated around the frontal structural members and their connections to the main chassis. Comparison of the model-wide maximum stress-time histories showed that the higher-speed simulation produced a larger and earlier recorded stress peak. These findings identify structural regions that warrant further investigation, although the numerical results alone do not establish the chassis's crashworthiness performance or its ability to protect occupants.

Several modelling limitations restrict the quantitative interpretation of these findings. The simplified chassis-only geometry excludes wheels, suspension components, batteries, body panels, and occupants, while the idealised structural connections and frictionless contact conditions do not fully represent real-world vehicle behaviour. Furthermore, the maximum total displacement includes rigid-body translation and rotation and cannot be directly interpreted as chassis crushing or passenger-compartment intrusion. The unusually high equivalent von Mises stresses also require verification of the material representation, particularly its treatment of plastic deformation and strain-rate effects. The absence of quantified energy absorption, contact forces, and occupant-compartment intrusion prevents a comprehensive assessment of structural crash performance.

Future investigations should prioritise verification of the constitutive material model, including appropriate elastoplastic behaviour, strain-rate sensitivity, and failure criteria where applicable. Additional mesh-convergence and energy-balance assessments should be performed to establish numerical reliability, while structural deformation should be distinguished from rigid-body motion through suitable relative-displacement measurements. Subsequent studies should incorporate more representative vehicle components, examine passenger-compartment intrusion and energy absorption at both impact velocities, and compare the numerical predictions with experimental observations or established crashworthiness benchmarks. These improvements would provide a stronger basis for evaluating frontal impact performance and investigating modifications to the chassis's principal load-transfer regions.

REFERENCES

1. Abramowicz, W. (2003). Thin-walled structures as impact energy absorbers. *Thin-Walled Structures, 41*(2–3), 91–107. https://doi.org/10.1016/S0263-8231(02)00082-4
2. Baroutaji, A., Sajjia, M., & Olabi, A. G. (2017). On the crashworthiness performance of thin-walled energy absorbers: Recent advances and future developments. *Thin-Walled Structures, 118*, 137–163. https://doi.org/10.1016/j.tws.2017.05.018
3. Baykasoğlu, C., Baykasoğlu, A., & Çetin, M. T. (2019). A comparative study on crashworthiness of thin-walled tubes with functionally graded thickness under oblique impact loadings.

International Journal of Crashworthiness, 24(4), 453–471. https://doi.org/10.1080/13588265.2018.1478775

4. Chandran, N., & Brahmachari, S. K. (2015). Technology, knowledge and markets: Connecting the dots—Electric rickshaw in India as a case study. *Journal of Frugal Innovation, 1*, 3. https://doi.org/10.1186/s40669-015-0003-5
5. Cochrane, C., Muneer, T., & Fraser, B. (2019). Design of an electrically powered rickshaw, for use in India. *Energies, 12*(17), 3346. https://doi.org/10.3390/en12173346
6. Danielson, K. T. (2022). Curved node-to-face contact schemes for higher-order finite elements in lumped-mass explicit methods. *Computer Methods in Applied Mechanics and Engineering, 395*, 115056. https://doi.org/10.1016/j.cma.2022.115056
7. Doley, D., Maurya, A. K., & Nama, S. (2023). Sustainability and safety implications of electric three-wheeler paratransit modes: A critical literature review on E-rickshaws. *Proceedings of the Eastern Asia Society for Transportation Studies, 14*, Paper PP3572. https://easts.info/on-line/proceedings/vol.14/pdf/PP3572.pdf
8. Gabauer, D. J., & Juengprasertsak, S. (2022). Examination of current MASH occupant compartment intrusion limits using real-world crash data. *Transportation Research Record, 2676*(6), 413–423. https://doi.org/10.1177/03611981221074646
9. Huh, H., & Kang, W. J. (2002). Crash-worthiness assessment of thin-walled structures with the high-strength steel sheet. *International Journal of Vehicle Design, 30*(1–2), 1–21. https://doi.org/10.1504/IJVD.2002.002022
10. Kovandová, H., Krejčí, J., & Kovanda, J. (2013). Crash tests of vehicles: Selected experiments and analysis. *Transactions on Transport Sciences, 6*(4), 193–202. https://doi.org/10.2478/v10158-012-0047-7
11. Marzbanrad, J., Alijanpour, M., & Kiasat, M. S. (2009). Design and analysis of an automotive bumper beam in low-speed frontal crashes. *Thin-Walled Structures, 47*(8–9), 902–911. https://doi.org/10.1016/j.tws.2009.02.007
12. Noorsumar, G., Rogovchenko, S., Robbersmyr, K. G., & Vysochinskiy, D. (2022). Mathematical models for assessment of vehicle crashworthiness: A review. *International Journal of Crashworthiness, 27*(5), 1545–1559. https://doi.org/10.1080/13588265.2021.1929760
13. Priye, S., & Manoj, M. (2020). Exploring usage patterns and safety perceptions of the users of electric three-wheeled paratransit in Patna, India. *Case Studies on Transport Policy, 8*(1), 39–48. https://doi.org/10.1016/j.cstp.2020.01.001
14. Reddy, T. J., Rao, Y. V. D., & Narayanamurthy, V. (2018). Thin-walled structural configurations for enhanced crashworthiness. *International Journal of Crashworthiness, 23*(1), 57–73. https://doi.org/10.1080/13588265.2017.1306824
15. Salagame, R. R., & Belegundu, A. D. (1994). Distortion, degeneracy and rezoning in finite elements—A survey. *Sadhana, 19*(2), 311–335. https://doi.org/10.1007/BF02811901
16. Schmucker, U., Dandona, R., Kumar, G. A., & Dandona, L. (2011). Crashes involving motorised rickshaws in urban India: Characteristics and injury patterns. *Injury, 42*(1), 104–111. https://doi.org/10.1016/j.injury.2009.10.049

17. Singh, R., Mishra, S., & Tripathi, K. (2021). Analysing acceptability of E-rickshaw as a public transport innovation in Delhi: A responsible innovation perspective. *Technological Forecasting and Social Change, 170*, 120908. https://doi.org/10.1016/j.techfore.2021.120908